

Spectral Characteristics of Motion Artifacts in Wireless ECG and their Correlation with Reference Motion Sensors

Jannis Lilienthal, and Waltenegus Dargie, *Senior Member, IEEE*

Abstract—The increasing population size of the elderly is fostering the development of telehealth and assisted living systems. In this respect, monitoring vital biophysical conditions using wireless devices, such as the wireless electrocardiogram (WECG), plays a pivotal role in telemonitoring. However, the freedom of movement brings with it motion artifacts, the magnitude of which can be significant enough to interfere with the cardiac signals. To reason about and remove the artifacts, reference models (signals) are needed. In the context of WECGs, one way to construct these models is to employ motion sensors that can pick up the motion affecting the electrodes of the WECGs. In this paper, we experimentally examine the spectra of motion artifacts and the existence of correlations between inertial sensors and motion artifacts. We make use of three different types of sensors (3D accelerometer, 3D gyroscope, and skin-electrode impedance sensor) to assess the characteristics of different movement types. We found that the spectra of motion artifacts are determined by the type of movement. While lower-intensity motion artifacts (e.g., bending forward) are most pronounced below 2 Hz, others (e.g., running) manifest themselves in a series of distinct peaks between 1–10 Hz.

Index Terms—accelerometer, electrocardiogram, gyroscope, inertial sensor, motion artifacts, skin-electrode impedance, tele-monitoring

I. INTRODUCTION

The electrocardiogram (ECG) is widely used to diagnose and monitor Cardiovascular diseases (CVDs). Its wireless version can be useful for monitoring patients in their residential settings [1], [2]. One of the challenges associated with the employment of such devices is the existence of motion artifacts that can be significant enough to interfere with cardiac signals and, hence, impede their evaluation, both manual and automatic.

Different approaches have been proposed to reason about and remove artifacts. Among the techniques belong independent component analysis [3], tensor decomposition [4], wavelet denoising [5] and adaptive filtering [6]. As far as their characterization is concerned, Buxi et al. [7] investigated the correlation between motion artifacts and electrode-skin impedance for various motion types. The authors' measurement setup was based on capturing an ECG signal at the back of a subject, assuming that cardiac influence is negligible there. The different activities performed to generate artifacts were divided into (1) local skin artifacts (push/pull electrode, stretch/twist skin) and (2) global artifacts (Walking, Running, Jumping). Their results suggest that measurements pertaining

to the variation in the electrode-skin impedance can serve as a reference signal for the reduction of motion artifacts (for example, in adaptive filtering). However, their study is missing a comparison with inertial measurements. Furthermore, even though the activities causing global artifacts were of high intensity, they, nevertheless, were performed on the spot, thus not representing actual daily motions.

Cömert et al. [8] examined the spectral characteristics of the electrode-skin impedance for textile electrodes. The authors simultaneously measured the impedance at eight different current frequencies while applying a controlled motion sequence and specific magnitudes of force on the electrodes. Their findings suggest that if the aim is to detect or reduce motion artifacts, impedance frequencies should not be used within the range of biosignals (i.e., ECG and EMG that are below 500 Hz). The authors propose to use frequencies between 17 kHz and 1 MHz instead since artifacts and motion reference correlate best there.

The human movement is composed of complex and highly coordinated mechanical interactions of the musculoskeletal system. Muscles generate forces and apply moments to joints to provide static and dynamic stability to the body. Many gait parameters change with increasing speed, including step length, cycle duration, and muscle activation intensity. Although walking and running share some fundamental kinetics and kinematics, they are also distinctly different. In fact, both kinematics and kinetics change abruptly from a walking gait to a running gait [9].

How these properties translate into the generation of motion artifacts in ECG has not been thoroughly studied. Characterizing the spectral properties of motion artifacts has so far been limited to Thakor et al. [10] who investigated the spectra for running on a treadmill only. In this paper, we investigate:

- the spectral characteristics of motion artifacts for various movement types, and;
- how these characteristics translate to the correlation between the measurements of different reference sensor types and motion artifacts.

The remaining part of this paper is organized as follows: In Section II we describe our measurement setup, including the movement types considered and the equipment employed. In Section III we analyze the spectral properties for different movement types. In Section IV we analyze how these characteristics translate to the correlation between reference sensors and motion artifacts. Closing with Section V where we provide concluding remarks.

J. Lilienthal, and W. Dargie are with the Technische Universität Dresden, Germany (e-mail: jannis.lilienthal@tu-dresden.de; waltenegus.dargie@tu-dresden.de)

This work has been funded by the German Research Foundation (DFG) under the project agreements DA 1211/7-1 (RoReyBaN).

II. MATERIAL AND METHODS

To measure cardiac action potentials and physical exertions, we employed the Shimmer3 platform [11], which consists of a wireless electrocardiogram (WECG), a 3D accelerometer, and a 3D gyroscope, among others. In addition, the platform integrates two ADS1292R chips (Texas Instruments), enabling the simultaneous measurement of the ECG and skin-electrode impedance ($f_{mod} = 32$ kHz, and $I_{Imp} = 30$ μ A). Furthermore, all the available sensors can be sampled synchronously.

This study includes actual measurements taken from eleven healthy subjects (mean age = 30 yr, SD = 6 yr) performing the following activities: standing up from a chair, bending forward, walking, running, jumping on the spot and going up and down a flight of stairs. The list accommodates high impact motions (running, jumping, and climbing stairs) but also movements of moderate intensity (standing up, bending forward, and walking). Light activities were deliberately included as they are associated with elderly monitoring and independent living. The experimental procedures involving human subjects described in this paper were approved by the Institutional Review Board. One Shimmer3 node was attached at the center of the sternum of each subject to register movement and record the cardiac activity through a set of wet ECG electrodes (Kenndal, H135SG). The skin was prepared using alcohol wipes to clean the contact area, and all leads were fixed to the torso with surgical tape to minimize localized motion. Figure 1a illustrates the applied sensor arrangement.

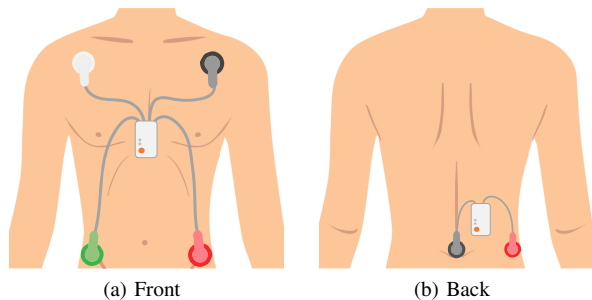


Fig. 1. Electrode and sensor location at the front and the back of the subjects.

An additional sensor node was placed at the back of each subject to capture the changes in the electrical potential caused by motion. The electrodes were placed at the high of the lumbar curve (cf. Fig. 1b), where cardiac influence is assumed to be negligible [7], [12]. The configuration was chosen to minimize the effect of cardiac action potentials and to maximize the impact of physical motion. By suppressing cardiac action potentials this way, it is possible to investigate the relationship between (a) the motion artifacts generated by motion alone and (b) the output of the motion sensors. Each movement was performed for two minutes to contain sufficient motion cycles for further analysis. The data were preprocessed following the recommendations for the standardization of the ECG made by the American Heart Association (AHA) [13]. Thereby the spectra of the signals was limited to 0.05–150 Hz.

Since the data analysis was performed offline, we employed zero-phase digital filtering by processing the raw data in both the forward and reverse directions (bi-directional filtering). This method prevents phase distortions from interfering with the outcomes of the correlation analysis. The outlined preprocessing procedure is equally applied to all the sensor data.

III. SPECTRAL CHARACTERISTICS OF MOTION ARTIFACTS

In the following chapter, we examine how the different mechanical properties of movements are reflected in the generation of artifacts. Therefore, we considered the isolated motion artifacts obtained from the back of each subject. After preprocessing, we extracted the power spectrum for each motion and subject and derived the relative power from it by normalizing the spectra to the range of 0 to 1. Figure 2 presents the mean value of the relative spectral power for artifacts produced by the six motions considered. Since the relative power of the spectra decreases for $f > 16$ Hz, these data are not shown here.

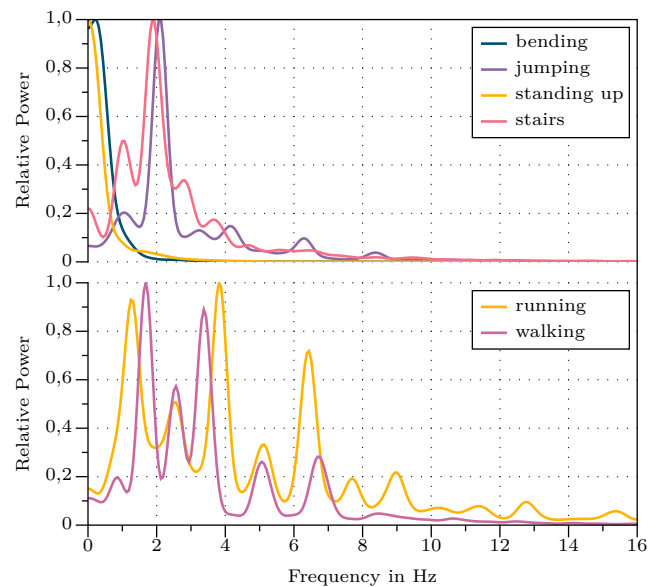


Fig. 2. Frequency spectrum of motion artifacts for different types of movements.

A cursory look suggests that the spectra for the exercises manifest distinctive characteristics at different frequency bands. According to these, the movements can be categorized into three groups: The first group contains bending and standing up, for which the relative power is concentrated in frequencies below 2 Hz. The second group is made up by jumping and going up and down a flight of stairs. For these movements, the motion artifacts exhibit a distinct peak around 2 Hz. The last group contains walking and running, for which the motion artifacts have a significantly more complex spectral composition. Their data show numerous peaks distributed over various frequencies.

The results indicate that motion artifacts markedly change their characteristics with a change in movement type. Bending forward and getting up from a chair are slowly executed movements where the relative power is highest in lower frequency bands. Both jumping and going up and down a flight of stairs feature distinctive frequency peaks around 2 Hz. Analyzing the accelerometer data for jumping suggests that these peaks likely correspond to the primary execution pattern (≈ 2 jumps per second). On the other hand, the spectrum for running is much more sophisticated in its composition, manifesting a series of characteristic peaks. This could result from the significantly more complex movement composition – combining forward and lateral direction patterns.

We conclude that there is no typical pattern to which all the motion artifacts adhere. Instead, they change their characteristics when the motion type changes. It is, therefore, necessary to take these characteristics into account when designing algorithms for motion artifact removal and applying them to corrupted signals.

IV. CORRELATION BETWEEN MOTION ARTIFACTS AND REFERENCE SENSORS

A. Motion Sensors vs. Isolated Artifacts

In the following, we intend to determine the extent to which specific frequencies contribute to the correlation between reference sensors and artifacts. Because many algorithms [4], [6], [12] rely on this correlation, its characteristics and strength determine the performance in artifact removal.

In order to analyze the correlation between specific frequency bands of two time series, the data must be decomposed into their constituting frequency elements first. Therefore, we applied the continuous wavelet transform (CWT) [14] on the ECG and the inertial sensor data to transform them from time into the time-frequency space. Wavelet transforms employ a base function Ψ , which is stretched or compressed to capture low or high frequency components in the signal while preserving the temporal characteristics. As a mother wavelet, we selected the Morlet wavelet [15]. Each time series was transformed into 106 narrow frequency sub-bands. Subsequently, we determined the Pearson correlation

coefficient R_p between the respective frequency-constrained artifact and reference signals. Because the accelerometer and the gyroscope measure three-dimensional acceleration and rotational velocity, we selected the axis that correlates best with the isolated artifacts.

Figure 3a and 3b display the correlation between isolated frequency bands of motion artifacts and the inertial sensors. The movements can be categorized into two groups based on the frequency bands in which the correlation to reference sensors is strong. The first group, illustrated in Figure 3a, contains the movements bending, standing up, and climbing stairs. For these groups, the frequency range producing $R_p > 0.25$ are primarily concentrated below $f \approx 1.5$ Hz. There are no obvious characteristic points that stand out to neighboring frequencies. On the other hand, the inertial sensor data for jumping, walking and running (cf. Figure 3b) exhibit $R_p > 0.25$ for $f > 1$ Hz. Each of these movements reveals distinctive peaks distributed over a range of different frequencies (e.g., 1.5 Hz, 2.5 Hz). However, the correlation in frequencies below 1 Hz is limited for these movements.

B. Motion Sensors and the ECG

In this section, we limit our comparison to the strength of correlation between the ECG in motion (lead I), on the one hand, and the accelerometer, gyroscope, and impedance sensor in the sensor platform placed at the sternum, on the other.

The motion types can be categorized into two groups based on their frequency-dependent features – similar to the isolated artifacts addressed in the previous section. The first group contains the activities bending, stand up, and climbing stairs and is illustrated in the upper part of Figure 4. In these movements a correlation of a reliable degree ($R_p > 0.2$) can be observed for a frequency below ~ 1 Hz, but the values decline consistently for higher frequencies ($R_p \approx 0.15$ at 10 Hz). The movements belonging to the second group refer to walking, running, and jumping. For these movements, the values of the correlation coefficients are strongly frequency-dependent for all motion sensors. Unlike the first group, however, this group continues to exhibit distinct features in the remaining frequency ranges as well. Indeed, there exist

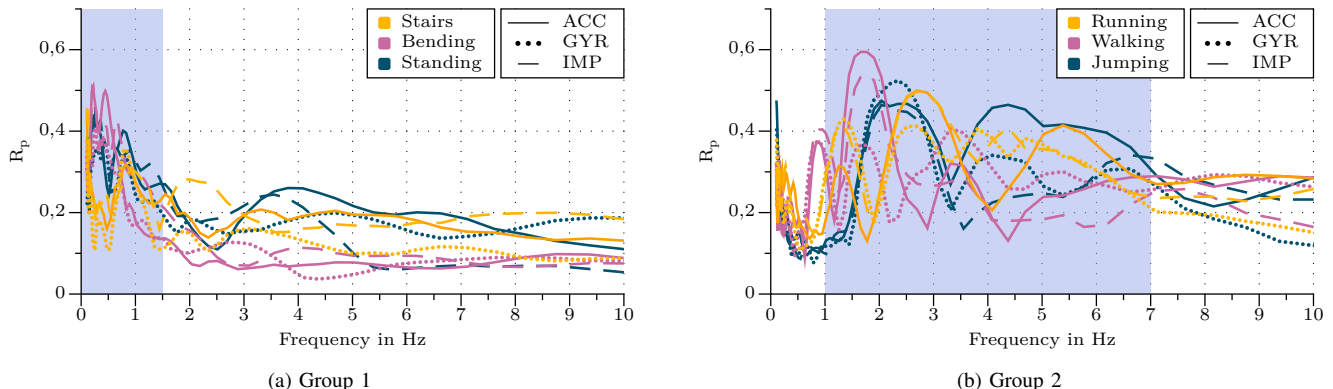


Fig. 3. Median Pearson correlation coefficient R_p depending on the frequency bands.

multiple peaks at various frequency points (e.g., 1.5 Hz and 4.5 Hz), thus revealing spectral bands in which the reference sensors and the ECG share mutual information.

To further study the relationship between motion and the resulting artifacts, we first employed a moving window cross-correlation (i.e., the correlation between two time-shifted signals) [7], [8]:

$$R_{xy}(m) = E[x_{n+m}y_n^*] \quad (1)$$

where E is the expected value and x and y are two time series. The cross-correlation was normalized so that the autocorrelations of x and y at zero lag are equal to one. Subsequently, the cross-correlation can attain values between -1 and 1. As part of our investigation, we examine the relation between motion artifacts and reference sensors under the best possible conditions. Therefore we employ the maximum absolute cross-correlation – $\max |\hat{R}_{xy,coeff}|$ having values between 0 and 1. We shall refer to it as: $|R|_{max,corr}$.

As Figure 5 reveals, the outputs of the different sensors score different correlation coefficients for almost all motion types (one exception is stair climbing). The accelerometer performs best in all the movement types save running and walking (where the gyroscope outperforms it). For standing up and climbing stairs, the correlation coefficients for all three sensors are small (none of the sensors score a correlation coefficient greater than 0.3). Figure 4 displays the median absolute correlation coefficient between the frequency bands of the ECG lead I and the reference sensors for frequencies lower than 10 Hz. The correlation for higher frequencies is not displayed here, as there are no distinct characteristic points, and the values are too small to be interesting. Because the skin-electrode impedance and the noisy ECG share distinctive characteristics, they will be addressed afterward.

So far, this data reveals that motion artifacts significantly change their properties with a change in motion. This is reflected in their spectra and the correlation to the accelerometer and the gyroscope. Even though bending and jumping achieve comparable cross-correlation levels, the nature of

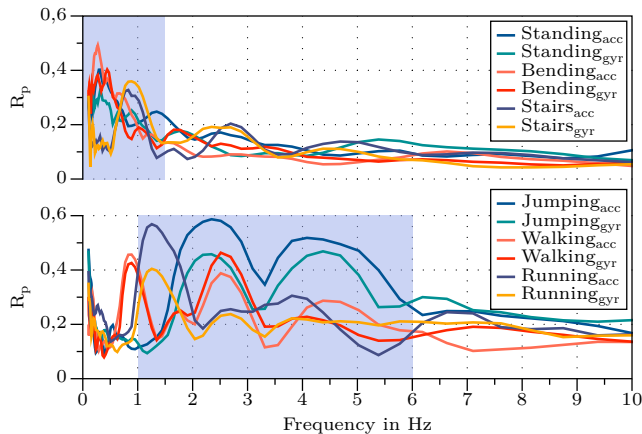


Fig. 4. Median correlation between the ECG and reference sensors depending on the frequency bands.

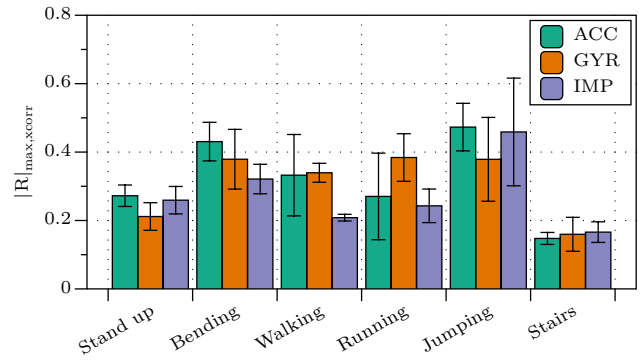


Fig. 5. Median of the maximum cross-correlation coefficient between different sensor types and the ECG-lead I.

the underlying frequencies contributing to this relation is divergent.

Figure 6 displays the correlation between the ECG and the skin-electrode impedance sensor. The accelerometer and the skin-electrode impedance sensor at the back serve as a reference. As can be seen, the impedance sensor correlates with the ECG, compared to the inertial sensors, over a broader range of frequencies. At the same time, similar to the inertial sensors, it also exhibits a strong correlation below 6 Hz. For all types of movements, the correlation steadily increases from 6 Hz to about 17 Hz, but steadily declines afterward, reaching a local minimum at 30 Hz. Neither the impedance sensor at the back nor the acceleration sensor shows similar characteristics.

In the range between 6–30 Hz, the impedance is highly correlated with the ECG. Perhaps this is due to the existence of mutual cardiac components in both signals resulting from ventricular depolarizations. These bands are often chosen in the literature for detecting the R-peaks in the ECG signal (refer to [16]). Moreover, in impedance cardiography, the bioimpedance is used, with a different electrode configuration, to capture cardiac features such as stroke volume and heart rate [17]. Therefore it is likely that cardiac activities influence the impedance readouts in the employed setup. Figure 7 depicts the data from the ECG of lead I, the preprocessed impedance, and the preprocessed ECG for one subject performing the movement bending. The impedance and the

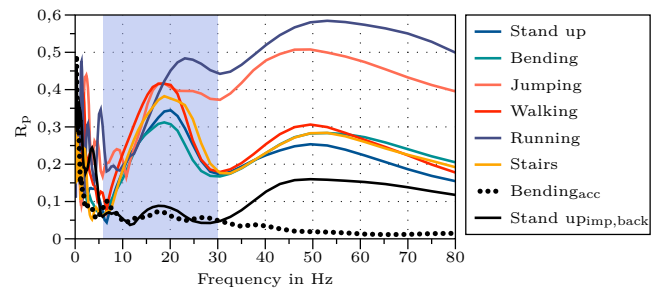


Fig. 6. Median correlation between the ECG, the impedance and accelerometer depending on the frequency bands.

ECG were preprocessed to emphasize cardiac activity (the R-peak). Both signals were bandpass filtered (8–20 Hz) using cutoff frequencies often applied in QRS-Detection algorithms (refer to [16]). We preprocessed the data according to common practices in QRS-Detection (squaring, differentiating, moving mean – cf. [18]). The times of the occurrence of the R-peaks extracted from the ECG match the respective patterns in the impedance. Therefore, the correlation in the sub-bands from 6–30 Hz is likely resulting from the impedance picking up cardiac activities.

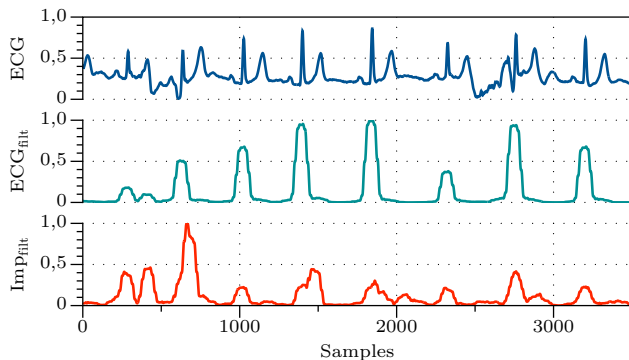


Fig. 7. Comparison of the ECG and the impedance.

V. CONCLUSION

In this paper, we investigated the spectra of motion artifacts and their correlation to reference sensors. We found that motion artifacts greatly vary in their characteristics, subject to a change in motion. Lower intensity movements generate motion artifacts concentrating in lower frequency bands. On the other side, movements associated with gait dynamics evoke artifacts that are significantly more complex in their composition.

These findings are consistent with their correlation to reference sensors. Bending, stand up, and climbing stairs manifest correlations in sub-bands below 1.5 Hz. However, for jumping, running, and walking, a stable correlation can be observed for frequencies in the useful ECG bands applied to detect the QRS-complex.

This seems to suggest that when developing techniques to remove motion artifacts from the ECG, the type of movements should be carefully considered in the analysis to reflect their characteristics. Although accelerometers and skin-electrode impedance experience similar levels of correlation, the nature of the underlying frequencies is divergent. Besides a stable and appreciable correlation in the lower frequencies, the impedance exhibits a high correlation in frequency bands commonly used to detect heartbeats in the ECG. Therefore, when using the change in the skin-electrode impedance as a reference, the frequency range should be carefully chosen to avoid removing cardiac information from the ECG.

REFERENCES

[1] C. Bruser, C. H. Antink, T. Wartzek, *et al.*, “Ambient and Unobtrusive Cardiorespiratory Monitoring Techniques,” *IEEE Reviews in Biomedical Engineering*, vol. 8, pp. 30–43, 2015.

[2] U. Satija, B. Ramkumar, and M. Sabarimalai Manikandan, “A Review of Signal Processing Techniques for Electrocardiogram Signal Quality Assessment,” *IEEE Reviews in Biomedical Engineering*, vol. 11, pp. 36–52, 2018.

[3] P. Mishra and S. K. Singla, “Artifact Removal from Biosignal using Fixed Point ICA Algorithm for Pre-processing in Biometric Recognition,” *Measurement Science Review*, vol. 13, no. 1, pp. 7–11, Jan. 2013.

[4] J. Lilienthal and W. Dargie, “Application of Tensor Decomposition in Removing Motion Artifacts from the Measurements of a Wireless Electrocardiogram,” *FUSION 2020 - 23rd International Conference on Information Fusion*, no. May, 2020.

[5] S. Nagai, D. Anzai, and J. Wang, “Motion artefact removals for wearable ECG using stationary wavelet transform,” *Healthcare Technology Letters*, vol. 4, no. 4, pp. 138–141, Aug. 2017.

[6] R. Qureshi, M. Uzair, and K. Khurshid, “Multistage Adaptive filter for ECG signal processing,” *Proceedings of 2017 International Conference on Communication, Computing and Digital Systems, C-CODE 2017*, no. January, pp. 363–368, 2017.

[7] D. Buxi, S. Kim, N. Van Helleputte, *et al.*, “Correlation between electrode-tissue impedance and motion artifact in biopotential recordings,” *IEEE Sensors Journal*, vol. 12, no. 12, pp. 3373–3383, 2012.

[8] A. Cömert and J. Hyttinen, “Impedance spectroscopy of changes in skin-electrode impedance induced by motion,” *BioMedical Engineering Online*, vol. 13, no. 1, p. 149, 2014.

[9] G. Cappellini, Y. P. Ivanenko, R. E. Poppele, *et al.*, “Motor patterns in human walking and running,” *Journal of Neurophysiology*, vol. 95, no. 6, pp. 3426–3437, 2006.

[10] N. V. Thakor, J. G. Webster, and W. J. Tompkins, “Estimation of QRS Complex Power Spectra for Design of a QRS Filter,” *IEEE Transactions on Biomedical Engineering*, vol. BME-31, no. 11, pp. 702–706, Nov. 1984.

[11] A. Burns, B. R. Greene, M. J. McGrath, *et al.*, “SHIMMER - A wireless sensor platform for noninvasive biomedical research,” *IEEE Sensors Journal*, vol. 10, no. 9, pp. 1527–1534, Sep. 2010.

[12] I. Romero, D. Geng, and T. Berset, “Adaptive filtering in ECG denoising: A comparative study,” *Computing in Cardiology*, vol. 39, pp. 45–48, 2012.

[13] P. Kligfield, L. S. Gettes, J. J. Bailey, *et al.*, “Recommendations for the Standardization and Interpretation of the Electrocardiogram,” *Circulation*, vol. 115, no. 10, pp. 1306–1324, Mar. 2007.

[14] C. E. Heil and D. F. Walnut, “Continuous and discrete wavelet transforms,” *SIAM Review*, vol. 31, no. 4, pp. 628–666, Dec. 1989.

[15] D. Morlet, F. Peyrin, P. Desseigne, *et al.*, “Time-scale analysis of high-resolution signal-averaged surface ECG using wavelet transformation,” in *[1991] Proceedings Computers in Cardiology*, IEEE Comput. Soc. Press, 1992, pp. 393–396.

[16] M. Elgendi, M. Jonkman, and F. Deboer, “Frequency bands effects on QRS detection,” *BIO SIGNALS 2010 - Proceedings of the 3rd International Conference on Bio-inspired Systems and Signal Processing, Proceedings*, no. June, pp. 428–431, 2010.

[17] J.-L. Fellahi and M.-O. Fischer, “Electrical Bioimpedance Cardiography: An Old Technology With New Hopes for the Future,” *Journal of Cardiothoracic and Vascular Anesthesia*, vol. 28, no. 3, pp. 755–760, Jun. 2014.

[18] J. Pan and W. J. Tompkins, “Real-Time QRS Detection Algorithm,” *IEEE Transactions on Biomedical Engineering*, vol. BME-32, no. 3, pp. 230–236, 1985.